11-2015

DNA-Mediated Excitonic Upconversion FRET Switching

Donald L. Kellis
Boise State University

Sarah M. Rehn
Boise State University

Brittany L. Cannon
Boise State University

Paul H. Davis
Boise State University

Elton Graugnard
Boise State University

See next page for additional authors

Publication Information

Kellis, Donald L.; Rehn, Sarah M.; Cannon, Brittany L.; Davis, Paul H.; Graugnard, Elton; Lee, Jeunghoon; Yurke, Bernard; and Knowlton, William B. (2015). "DNA-Mediated Excitonic Upconversion FRET Switching". *New Journal of Physics, 17*, 115007-1 - 115007-11. https://doi.org/10.1088/1367-2630/17/11/115007

New Journal of Physics
The open access journal at the forefront of physics

Deutsche Physikalische Gesellschaft DPG
IOP Institute of Physics

Published in partnership with: Deutsche Physikalische Gesellschaft and the Institute of Physics

OPEN ACCESS

RECEIVED
2 September 2015

REVISED
13 October 2015

ACCEPTED FOR PUBLICATION
20 October 2015

PUBLISHED
17 November 2015

PAPER

DNA-mediated excitonic upconversion FRET switching

Donald L Kellis[1], Sarah M Rehn[2], Brittany L Cannon[1], Paul H Davis[1], Elton Graugnard[1], Jeunghoon Lee[1,2], Bernard Yurke[1,3] and William B Knowlton[1,3]

[1] Department of Materials Science and Engineering, Boise State University, Boise, ID 83725, USA
[2] Department of Chemistry and Biochemistry, Boise State University, Boise, ID 83725, USA
[3] Department of Electrical and Computer Engineering, Boise State University, Boise, ID 83725, USA

E-mail: jeunghoonlee@boisestate.edu, bernardyurke@boisestate.edu and bknowlton@boisestate.edu

Keywords: upconverting nanoparticles, FRET, DNA nanotechnology, excitonics, strand displacement, excitonic switch

Supplementary material for this article is available online

Abstract

Excitonics is a rapidly expanding field of nanophotonics in which the harvesting of photons, ensuing creation and transport of excitons via Förster resonant energy transfer (FRET), and subsequent charge separation or photon emission has led to the demonstration of excitonic wires, switches, Boolean logic and light harvesting antennas for many applications. FRET funnels excitons down an energy gradient resulting in energy loss with each step along the pathway. Conversely, excitonic energy upconversion via upconversion nanoparticles (UCNPs), although currently inefficient, serves as an energy ratchet to boost the exciton energy. Although FRET-based upconversion has been demonstrated, it suffers from low FRET efficiency and lacks the ability to modulate the FRET. We have engineered an upconversion FRET-based switch by combining lanthanide-doped UCNPs and fluorophores that demonstrates excitonic energy upconversion by nearly a factor of 2, an excited state donor to acceptor FRET efficiency of nearly 25%, and an acceptor fluorophore quantum efficiency that is close to unity. These findings offer a promising path for energy upconversion in nanophotonic applications including artificial light harvesting, excitonic circuits, photovoltaics, nanomedicine, and optoelectronics.

1. Introduction

In many nanophotonic systems, excitons are funneled down an energy gradient created by an array of fluorophores possessing successively lower excitation energies. Examples of such excitonic systems include light harvesting antennae in higher plants [1, 2], certain bacteria [3, 4], synthetic waveguides [5, 6], switches, and logic gates [7–9]. The energy is degraded due to losses at each step in the exciton transfer process, limiting the performance of exciton funnels. This degradation raises the question of whether the exciton funnel performance can be improved via an upconversion process in which two excitons combine to form a single exciton of higher energy, thus rejuvenating the exciton energy. Indeed, nature appears to have taken this approach, as energy upconversion has been observed in the energy transfer pathways present within the Fenna–Mathews–Olson [10–12] complexes of natural photosynthetic systems [13, 14]. Optical upconversion also occurs in lanthanide-doped materials such as $NaYF_4$:Gd^{3+}, Yb^{3+}, Er^{3+}, both in bulk solid crystals and nanoparticles; however, the upconversion process in these materials differs mechanistically from the natural upconversion phenomenon [15, 16]. Although inherently inefficient, the efficiencies of upconversion nanoparticles (UCNPs) continue to improve [17], which offers an opportunity to pursue energy upconversion in artificial excitonic systems including excitonic wires, switches, and light harvesting antennae. UCNPs are being explored in the biomedical field as alternatives or supplements to current imaging agents, bioassays, and drug delivery modalities because of their narrow bandwidth emission, near zero autofluorescence, low toxicity, deep tissue penetrating near infrared (NIR) excitation, and minimal photobleaching [16, 18–24]. Additionally, UCNPs are currently studied as potential components in optoelectronic applications such as light-emitting diodes [25], fluorescent lighting [26], telecommunications [27], security coatings [23, 24], and photovoltaic devices [28, 29]. Further

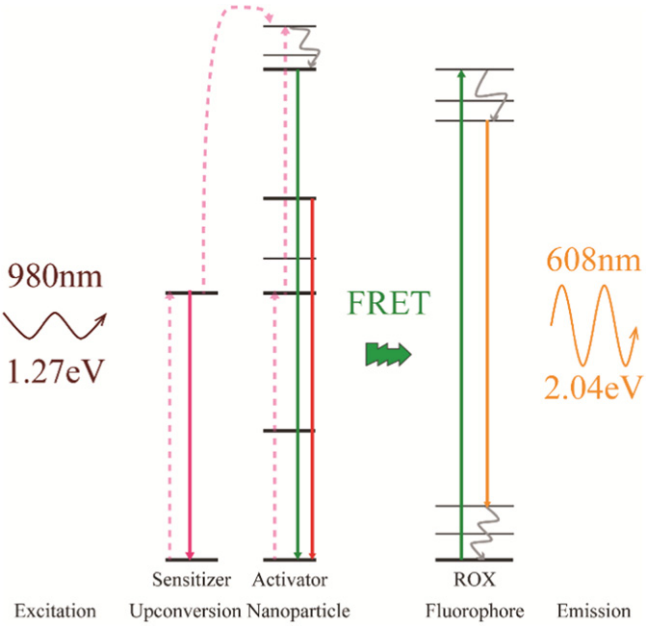

Figure 1. Schematic illustration of optical upconversion followed by FRET for a donor (UCNP)/acceptor (fluorophore) pair. The donor UCNP undergoes a multi-step energy transition upon low energy near infrared (NIR) excitation as detailed in various review publications [15–17, 27, 33, 41]. Upon relaxation to the ground state, the UCNP non-radiatively transfers its energy via dipole–dipole interactions (FRET) to an acceptor molecule (fluorophore). This process results in emission of a photon from the acceptor.

development of UCNP systems may provide significant advancements in these nanomedicine and optoelectronics applications.

Combining optical upconversion and Förster resonance energy transfer (FRET) can create new hybrid UCNP systems affording production of novel bioanalytical tools [30] and improve device functionality in optoelectronics applications [31, 32]. Upconversion in lanthanide-doped nanoparticles is a nonlinear optical phenomenon achieved through the excitation of rare earth ions by two or more lower energy NIR photons, resulting in multistep electronic transitions followed by higher energy visible photon emission [27, 33, 34]. FRET is excitonic energy transfer on the nanometer scale between donor and acceptor molecules mediated by dipole–dipole coupling [35, 36]. The acceptor molecule need not be a fluorophore, and the energy transferred need not be radiated as fluorescence [37–39]. Though there are multiple ways in which combined upconversion and FRET systems can be constructed, here the focus will be on FRET between a UCNP donor and an acceptor fluorophore. During FRET, the fluorescence from the donor UCNP decreases (i.e., a quenching effect) with a simultaneous increase in the acceptor molecule's fluorescence as the donor–acceptor pair are brought into proximity (i.e., a transfer effect) [40]. A simple schematic of the upconversion to FRET process is provided in figure 1, in which the sensitizer–activator complex provides the two photon absorption pathway within the UCNP [15–17, 33, 41], thereby initiating the FRET cascade from the UCNP to the fluorophore. In this report, we demonstrate the upconversion of incident infrared photons in $NaYF_4$:Gd^{3+}, Yb^{3+}, Er^{3+} nanoparticles followed by excitonic transfer (i.e., FRET) to fluorophores that emit photons in the visible region, that can be dynamically switched 'ON' and 'OFF'. Switching is accomplished via DNA hybridization and toehold-mediated DNA strand-displacement reactions [42], in which auxiliary DNA oligomers attached to the UCNPs are used to control subsequent reversible binding of DNA oligomers carrying the fluorophores to the nanoparticle.

Spectral overlap between the donor emission and the acceptor absorption and donor–acceptor distance are the two key components required for efficient FRET. In an ideal FRET process, such as that depicted in figure 2(a), complete nonradiative energy transfer between the donor and acceptor occurs (dashed curve). This energy transfer can be maximized by optimizing the spectral overlap and reducing the distance between the donor and acceptor to maximize FRET. More typically, competing parasitic processes such as bleed-through, cross-talk, internal energy loss, and donor emission into free space decrease FRET efficiency (solid curve, figure 2(a)). As defined by Berney and Danuser [43], cross-talk occurs when the donor emission spectrum overlaps that of the acceptor emission, thereby artificially increasing the apparent acceptor emission signal. Cross-talk [21–23] can be virtually eliminated through the careful selection of the fluorophore acceptor such that its emission does not overlap that of the donor. Conversely, bleed-through [43] involves undesired excitation of the acceptor molecule at the donor excitation wavelength. An advantage to UCNP-fluorophore FRET systems, bleed-through is eliminated completely because the excitation wavelength of the UCNP donor

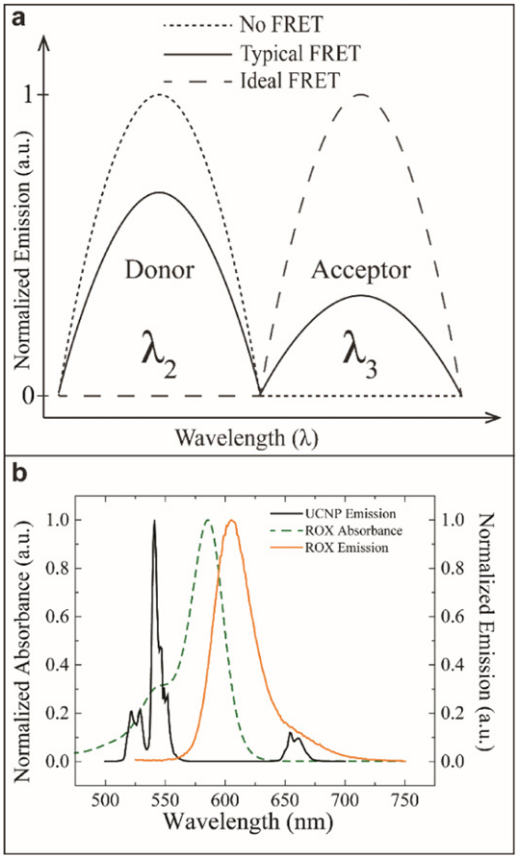

Figure 2. (a) Schematic of fluorescence emission spectra demonstrating: donor emission (1) without an acceptor present and thus zero FRET, (dotted line) or (2) in the presence of an acceptor, whereby the FRET process quenches the donor emission (λ_2) resulting in acceptor emission (λ_3) as occurs in typical FRET (solid line) and varies depending on FRET efficiency. If the FRET process approaches 100% transfer efficiency, and the acceptor has a fluorescence quantum yield of unity, near total quenching of the donor occurs and nearly 100% of the quanta absorbed by the donor are emitted as fluorescence photons by the acceptor (ideal FRET, dashed line). (b) Spectral overlap of the UCNP and ROX fluorophore. The emission spectrum of the $NaYF_4$ nanoparticle co-doped with Gd^{3+}, Yb^{3+}, Er^{3+} (black solid line) overlaps the shoulder of the ROX absorbance spectrum (green dashed line). The emission spectrum of ROX, which has minimal overlap with that of the UNCP emission, is also shown (orange solid line).

lies in the NIR spectrum, while the acceptor fluorophore excitation is in the visible. As a result, the incident UCNP excitation photons do not have sufficient energy to directly excite the acceptor fluorophore.

Figure 2(b) shows the relevant absorption and emission spectra of the FRET system components used in this study (i.e., spectral overlap). This system is composed of an upconverting $NaYF_4$ nanoparticle donor doped with Gd^{3+}, Yb^{3+}, Er^{3+} and a 6-carboxy-X-rhodamine (ROX) fluorophore acceptor bound to the UCNP via a hybridized DNA tether. Nanoparticle information, DNA sequences, and fluorophore details are provided in supplementary material S1. The low wavelength absorbance shoulder of the ROX acceptor coincides well with the emission peaks of the UCNP donor in the range of 515–562 nm, which provides adequate spectral overlap for FRET. Furthermore, cross-talk is minimized as the acceptor emission peak lies in a longer wavelength region than the donor emission resulting in virtually no cross-talk at the 608 nm peak ROX acceptor emission wavelength. It should be noted that some attenuation of the UCNP fluorescence in the range of 515–562 nm occurs when ROX is introduced, which will be discussed later. There is also potential cross-talk between the donor and acceptor in the 645–675 nm range; however, this spectral region falls well outside the spectral overlap region and does not contribute to the FRET. Thus, the unique optical properties of the UCNP donor and choice of ROX as the acceptor allow clear observation of donor quenching and acceptor emission in the spectral data.

There have been several reports of UCNP-fluorophore FRET systems [44–49], which have also been referred to as energy transfer [18, 50] or luminescence resonance energy transfer systems [51–56]. To the best of our knowledge, published investigations of UCNP-fluorophore FRET systems have primarily demonstrated one aspect of the FRET process, namely donor quenching [57–60], accompanied by a nominal increase in acceptor molecule emission suggesting an inefficient FRET process. In order for potential optoelectronic applications of UCNP-fluorphore FRET-based constructs, realization of higher efficiency FRET (figure 2(a)), in which both donor quenching and acceptor emission are significant, is an essential challenge that must be addressed.

2. Materials and methods

To address the primary challenge of hydrophobicity of as-synthesized lanthanide-doped UCNPs, biofunctionalization techniques [18] have been used such as PEGylation [61], oxidation [50], phospholipid coating [44], recombinant antibody fragment coating [46], aminoethyl dihydrogen phosphate [49], citrate capping [60], polyacrylic acid [62], streptavidin coating [53, 63], and silica shell growth [45, 64, 65]. These UCNP modification methods enable the use of acceptor molecules currently employed in the FRET process; however, these techniques potentially increase the UCNP dimensions [44] resulting in greater donor–acceptor pair separation distances, which decreases the FRET efficiency [58, 66]. Additionally, typical biofunctionalization methods, such as covalent lectin binding [57], covalent biotinylation [49, 50, 53, 63, 64], fluorophore incorporation within hydrophilic coatings [44, 61, 67, 68], amino group conjugation [45, 58], stain intercalation [52], covalent DNA immobilization [60], and covalent sulfhydryl linkage [69] involve multi-step processes. These multi-step biofunctionalization processes reduce overall yield and add complications to the UCNP preparation. Recently, a simple single-step ligand exchange method was reported by Li *et al* [70], in which single stranded DNA (ssDNA) was directly attached to the UCNP in a one step process, producing hydrophilic, monodispersed UCNPs for salt concentrations ranging from 5 to 100 mM. Subsequently, they were able to selectively attach a variety of ssDNA functionalized particles such as gold nanoparticles (AuNPs), Cy3 fluorophores, and cell targeting aptamers via Watson–Crick [71] hybridization to the available ssDNA. We believe this ssDNA functionalization method is advantageous for UCNP-based excitonic FRET because not only is it a single-step process, but additionally it reduces the donor–acceptor pair separation distance, thereby enhancing their FRET efficiency. Moreover, ssDNA functionalization enables the modulation of FRET through toehold-mediated strand-displacement reactions [42] when invasion (INV) and restoration (RES) ssDNA strands are introduced to perform UCNP-based FRET excitonic switching.

To explore the possibility of DNA-mediated UCNP-fluorophore FRET switching, four distinct challenges needed to be addressed: (i) rendering the hydrophobic UCNPs hydrophilic, (ii) functionalizing the hydrophilic UCNPs using the ssDNA biofunctionalization method, (iii) devising a FRET system, and (iv) designing a strand displacement sequence. Oleic acid capped, hydrophobic UCNPs were rendered both hydrophilic and functionalized with ssDNA, denoted as $UCNP_d$, via the one step ssDNA biofunctionalization method demonstrated by Li *et al* [70], as described in the supplementary material S2. In addition to imparting hydrophilicity, the ssDNA on the UNCP surface serve as tethers to which complementary ROX-functionalized ssDNA oligomers can hybridize. ROX was chosen as the acceptor because it can be readily attached to ssDNA and it provides adequate spectral overlap with the donor as discussed previously (figure 2(b)). The base sequences for the DNA strands involved in toehold-mediated strand displacement were designed using UNIQUIMER [72] software. UNIQUIMER employs random ssDNA sequence generation combined with parameters to control base pair (bp) length, complementarity, and C-G content of each strand. Thermodynamic analysis using the web-based NUPACK [73] program determined the free energy changes as each DNA oligomer (ROX, INV, or RES) hybridizes to its complement.

The scheme that was implemented to control the FRET between ssDNA functionalized $UCNP_d$ and the ROX fluorophore is illustrated in figure 3. The ROX fluorophore is covalently attached to a ssDNA oligomer complementary to a portion of the $UCNP_d$ ssDNA sequence; this ROX-DNA pair is referred to as ROX_a. Figure 3 (1) shows the $UCNP_d$ in the 'OFF' state where no ROX emission is observed. Switching to the 'ON' state occurs when the ROX_a hybridizes to the tether on the $UCNP_d$, as shown in (2). Here, the hybridization of the ROX_a strand to a 10 nucleotide (nt) toehold binding region (TH) on the $UCNP_d$ tether holds the ROX_a fluorophore in proximity to the $UCNP_d$, enabling FRET and the consequent ROX emission. Switching to the 'OFF' state is accomplished by displacement of the ROX_a from the donor with the introduction of a 22 nt invasion (INV) strand (3). Finally, restoration of the ROX_a strand to the $UCNP_d$, and thus reestablishing the 'ON' state, is achieved by addition of a 17 nt restoration (RES) strand displacing ROX_a by preferentially hybridizing with the INV strand (4). The process can be iterated to reversibly switch the system between the 'ON' and 'OFF' states (5). For the experiments described in this paper, the concentration of available DNA tethers was estimated to be $\sim$4 μM using the procedure described in supplementary material S2.3.

3. Results and discussion

The state of the FRET system was monitored in two ways after each switching event via fluorescence spectroscopy under conditions of continuous 980 nm excitation (instrumentation details provided in supplementary material S3). The emission intensity of the donor and the acceptor were acquired as a function of wavelength and time; the latter was performed at the peak emission wavelength of the ROX acceptor (608 nm). Figure 4 shows the normalized fluorescence spectra obtained for the 'OFF' and 'ON' states before and after

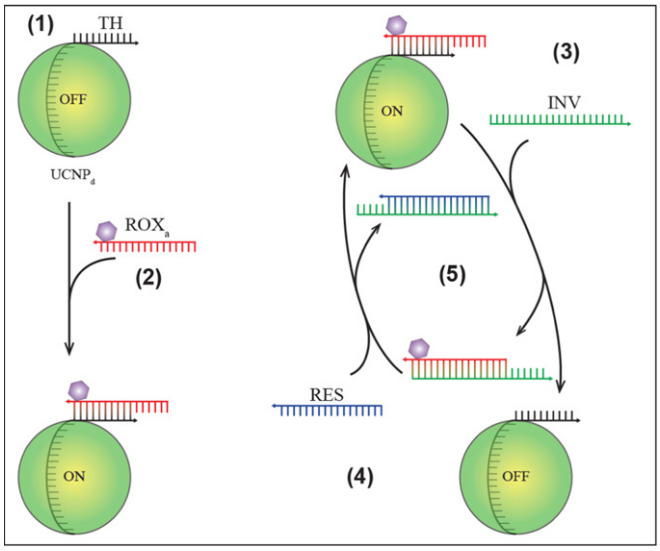

Figure 3. Diagram of the DNA-mediated excitonic upconversion FRET-based switching scheme. The initial state of the functionalized UCNP is shown at (1). The red ROX$_a$ strand hybridizes to a TH region of the black ssDNA attached to the UCNP$_d$, resulting in 'ON' state FRET emission (2). The green invasion strand (INV) interacts with a toehold region on the red ROX$_a$ strand, removing the acceptor from the donor (3), returning the donor to its original 'OFF' state. The blue restoration strand (RES) associates with a toehold region of the INV strand (4), freeing the red ROX$_a$ strand to reattach to the UCNP$_d$ and returning the system to its 'ON' state. Reversible switching is thus accomplished by repeatedly introducing the INV and RES strands (5).

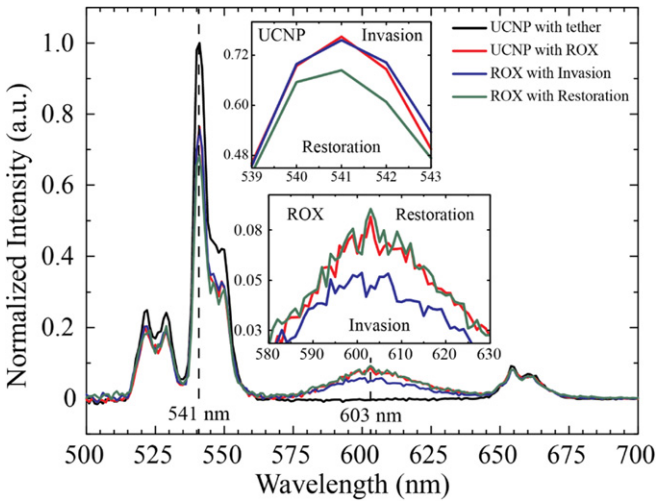

Figure 4. Normalized emission spectra of functionalized UCNPs under continuous 980 nm excitation. Hybridization of the ROX acceptor strand (step 2, figure 3) produced a decrease in the UCNP emission peaks in the range of 515–562nm coupled with a simultaneous increase in the ROX emission (red trace) in the range of 580–630 nm. Introduction of the ROX invasion strand (step 3, figure 3) induced a reduction of FRET (blue trace). Subsequent addition of the ROX restoration strand (step 4, figure 3) increased ROX emission (green trace), a signature of increased FRET and a demonstration of excitonic upconversion FRET switching. Spectra were collected approximately 30 min post interaction with the indicated strand. Interaction time is well beyond the calculated time to half completion of 120 $\pm$ 40 and 500 $\pm$ 120 s for the 'ON' and 'OFF' states, respectively, as described in the supplementary material S6.

addition of INV and RES strands to induce one cycle of excitonic switching. The normalization process is described further in supplementary material S4. As a control, the initial emission spectrum of the UCNP$_d$ in the absence of ROX$_a$ is shown as the black curve in figure 4.

The red curve in figure 4 shows that once the ROX$_a$ strand attaches to the UCNP$_d$, a clear decrease in the donor emission peaks in the range of 515–562 nm and a concomitant increase in the acceptor emission in the range of 580–630 nm, indicating FRET from the donor (upper inset) to the acceptor (lower inset). To our knowledge, such a significant and pronounced increase in acceptor fluorescence has not been previously observed in the published studies of lanthanide-doped UCNPs [44, 45, 50, 60, 61]. In these prior works, acceptor emission was either not observed or was nominal. We attribute the clear acceptor emission increase demonstrated in figure 4 to the shorter donor–acceptor (i.e., UCNP to ROX) distance arising from the direct

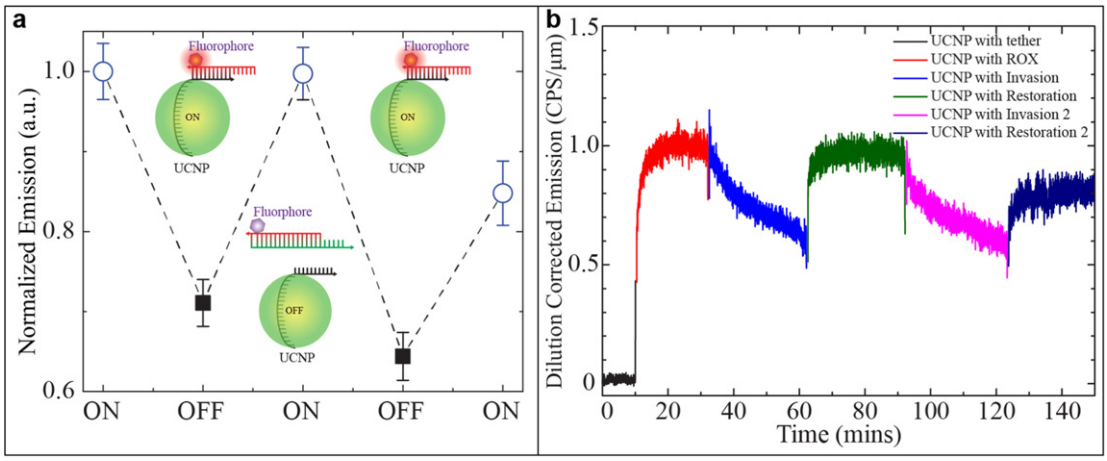

Figure 5. (a) Dynamic 608 nm emission of the DNA functionalized donor UCNP ($UCNP_d$) upon 980 nm excitation via hybridization of the fluorophore acceptor (ROX_a) labeled ssDNA. Cycling of the emission intensity by switching between 'ON' (blue circle) and 'OFF' (black square) states was achieved through toehold-mediated strand-displacement of the ROX_a strand. The lines between data points are provided for clarity and error bars represent three switching trials. (b) Dilution corrected reactions kinetics fluorescence data recorded at 608 nm. The excitation wavelength was 980 nm.

DNA functionalization method [70]. Although removal of the ROX_a (step 3, figure 3) by addition of INV strand only resulted in partial recovery of the donor emission peaks in the range of 515–562 nm to their original values, a simultaneous significant reduction (i.e., quenching) in the 608 nm acceptor emission peak was noted (lower inset blue curve). The partial recovery of the donor emission peaks in the range of 515–562 nm is most likely due to the incomplete removal of ROX_a from the $UCNP_d$, as evidenced by the incomplete quenching of the 608 nm acceptor emission. Analysis of the area containing the donor emission peaks was performed by integrating from of 500 to 562 nm and revealed values consistent with expected changes (supplementary material S13). The subsequent addition of the ROX restoration strand (step 4, figure 3) returns the ROX_a emission to the values of the green curve indicated in figure 4. To demonstrate the repeatability of this switching, the 'OFF–ON' cycle was iterated again resulting in spectra similar to the blue and green curves in figure 4 (raw emission spectra of all three cycles are provided in supplementary material S5).

Isothermal dynamic switching of FRET between $UCNP_d$ and ROX_a (i.e., induced acceptor emission changes at 608 nm as a function of time) is further highlighted in figures 5(a) and (b), which shows a series of successive switching events. Sequential and reversible switching between 'ON' and 'OFF' states is clearly demonstrated as evident by the saw-tooth pattern of figure 5(a), which is averaged over three trials. Stoichiometric dynamic switching was performed on 30 min intervals, figure 5(b). The average time to half-completion, as modeled by second-order kinetics for attachment ('ON' state) and removal ('OFF' state) of the ROX_a to the $UCNP_d$, were calculated to be 120 ± 40 s and 500 ± 120 s, respectively, at ~ 80 μM concentrations (data provided in supplementary material S6). As noted in figure 4 and observed in figures 5(a) and (b), the ROX_a emission at 608 nm does not return to zero in the 'OFF' state, which can most likely be attributed to the incomplete removal of the ROX_a strand from the $UCNP_d$ as discussed earlier. Except for the acceptor emission data (figures 4 and 5) in which the INV and RES strands were added in 1:1 stoichiometry, the acceptor emission does not noticeably decrease further upon application of INV strand in excess ratios (data not shown). Hence, it can be inferred that a substantial fraction of the initially supplied ROX_a is bound to the $UCNP_d$ in such a manner that it cannot be removed by strand invasion. Incomplete invasion due to oligomer crowding and direct adsorption of the ROX fluorophore to the surface of the $UCNP_d$ may explain why the 608 nm acceptor fluorescence does not return to zero in the switched 'OFF' state. Relative to the latter, we have found evidence of direct adsorption of the ROX fluorophore, or unspecific binding, when a control experiment was performed in which a mismatched sequence of the ssDNA ROX strand was used and added to a solution of $UCNP_d$ while monitoring the 608 nm acceptor emission (supplementary material S13). Nonetheless, the switching results demonstrated in figures 5(a) and (b) indicate that the toehold domains at least moderately retain their ability to perform the toehold-mediated strand-displacement reactions necessary for excitonic switching.

In order to compare this excitonic upconversion FRET system with other published work [44, 45, 50, 60, 61], the energy conversion efficiency (E_{con}) was determined. The E_{con} is defined as the ratio of the number of photons emitted by the acceptor in the presence of the donor to the number of photons emitted by the donor (UCNP) in the absence of the acceptor (fluorophore). This quantity is conveniently computed using the simple relationship:

Table 1. Comparison of UCNP-fluorophore systems.

Fluorophore	f_D	f_{AD}	E_{con}	Reference
TAMRA	14.6	1.23	0.08	[49]
BOBO3	20.9	0.84	0.04	[44]
RhB	19.4	2.35	0.12	[60]
TAMRA	20.0	2.80	0.14	[59]
RhB	18.2	1.44	0.08	[43]
ROX	13.5	3.07	0.23	this work

$$E_{con} = \frac{f_{AD}}{f_D}, \tag{1}$$

f_{AD} is the emission peak area of the fluorophore acceptor in the presence of the UCNP donor, and f_D is the emission peak area of the UCNP donor in the absence of the fluorophore acceptor. Data were extracted from the published spectra as described in supplementary material S7. The resulting E_{con} values were calculated, as summarized in table 1. The value of E_{con} for our system is 1.6 times greater than the next highest value [59]. This marked improvement in conversion efficiency occurs despite the reduction of spectral overlap between $UCNP_d$ and ROX_a compared to these other systems (supplementary material S8). We attribute the greater E_{con} in our system to the reduced donor–acceptor distance provided by the ssDNA direct attachment method. It is also possible that the lower E_{con} values observed for previous systems could result if the local chemical environment produced by the attachment chemistry increases nonradiative energy losses of either the donor or acceptor emission.

Further insight into the performance of the $UCNP_d$–ROX_a system can be obtained by considering two other quantities: the energy transfer efficiency (E_{trans}) [74] of the system and the quantum efficiency (Q_{eff}) [74–78] of the acceptor fluorophore. To define these quantities, in addition to f_D and f_{AD} already defined, we introduce f_A and f_{DA}, where f_A is the acceptor emission peak area in the absence of the UCNP donor and f_{DA} is the UCNP donor emission peak area in the presence of the acceptor. The E_{trans} is then given by

$$E_{trans} = 1 - \frac{f_{DA}}{f_D}. \tag{2}$$

E_{trans} is thus a measure of the relative decrease in UCNP donor fluorescence in the presence of the acceptor, with $E_{trans} = 1$ corresponding to complete (ideal, see figure 2(a)) FRET between the donor and acceptor; accordingly, E_{trans} is also occasionally referred to as the quenching efficiency [44, 74]. Assuming the decrease in the fluorescence of the donor in the presence of the acceptor is entirely due to the transfer of those photons to the acceptor, Q_{eff} is then given by

$$Q_{eff} = \frac{f_{AD} - f_A}{f_D - f_{DA}}. \tag{3}$$

Q_{eff} is a measure of the efficiency with which excitonic quanta transferred to the donor are converted into acceptor fluorescence photons and is thus a measure of the FRET acceptor's fluorescence quantum yield. For the $UCNP_d$–ROX_a system, direct excitation of the ROX_a by the infrared laser used to pump the $UCNP_d$ did not result in significant measurable ROX_a fluorescence, thus we can reasonably assume that $f_A = 0$ for this system (see supplementary material S9). Under these conditions, equations (1)–(3) yield:

$$E_{con} = Q_{eff} E_{trans}. \tag{4}$$

This decomposition of E_{con} provides a means of assessing the relative contributions to the conversion efficiency of two separate physical effects: exciton transfer from the donor to the acceptor and fluorescence emission of the acceptor.

A number of studies have been conducted to determine the Q_{eff} of ROX [75–78], all of which report values within the range of 1.0 ± 0.05 (i.e., unity quantum yield, within experimental uncertainty), indicating ROX is highly efficient at re-emission of absorbed photons. To calculate Q_{eff} of the $UCNP_d$–ROX_a system using equation (3), the donor emission peak areas from the spectra shown in figure 4 (black and red curves) were integrated from 514 to 562 nm, and the acceptor emission peak areas were integrated from 565 to 645 nm. Although minimal, it was necessary to consider the attenuation of the $UCNP_d$ in the presence of ROX_a. An attenuation correction factor $\left(f_D^C\right)$ was applied to our data prior to computing Q_{eff} and E_{trans} for our system to account for free ROX absorption, however, this could not be performed for the comparison to other published work (supplementary material S10). The Q_{eff} of this system calculated via equation (3) (1.08 ± 0.11) is unity within experimental uncertainty and falls within the range of the literature values for the quantum efficiency of

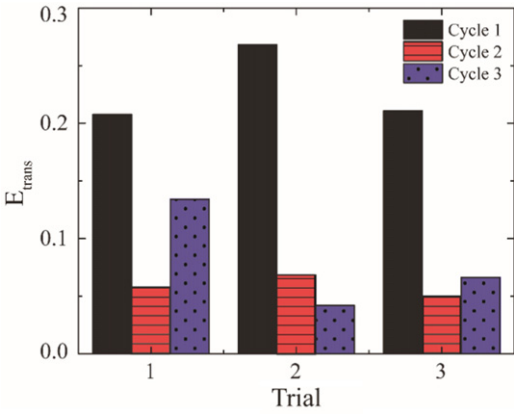

Figure 6. The energy transfer efficiency E_{trans} of the UCNP$_d$–ROX$_a$ system for three successive switching events observed in each of three trials. In the initial cycle, the system begins in the 'OFF' state in the absence of ROX$_a$. The ROX$_a$ is incompletely removed by the INV oligomer when restoring the system to the 'OFF' state in subsequent cycles. Hence, E_{trans} is lower for subsequent cycles because there are fewer active attachment sites for the ROX$_a$.

ROX. This result indicates that the excitonic coupling to the UCNP and attachment scheme adopted for ROX$_a$ have no observable detrimental effect on the Q_{eff} of ROX.

The energy transfer efficiency (E_{trans}) for the UCNP$_d$–ROX$_a$ system was evaluated using equation (2), where again peak areas from 514 nm to 562 nm and 565 nm to 645 nm were used to calculate the donor and acceptor emission, respectively. Black bars in figure 6 represent E_{trans} for the first 'OFF–ON' cycle evaluated for three separate trials.

The average value of E_{trans} for these three trials was 0.23 ± 0.03 (see supplementary material S11); note that since in our system Q_{eff} is close to unity, E_{trans} is essentially equal to E_{con} as shown in table 1. The nearly 25% energy transfer conversion efficiency is comparable to that of other UCNP FRET systems reported in the literature [44, 45, 50, 60, 61]. Figure 6 also displays E_{trans} evaluated for the second and third 'OFF–ON' cycles (red and blue bars) for each of the three trials. The combined average value of E_{trans} for all of the second and third 'OFF–ON' cycles is 0.07 ± 0.03. As already indicated, not all the ROX$_a$ is removed from the UCNP$_d$ by the INV oligomers used to transition the system from the 'ON' state to the 'OFF' state (see figure S3, supplementary material). Hence, after the first 'OFF–ON' cycle, there are fewer attachment sites to which ROX$_a$ (supplementary material S12) can bind; however these sites remain active on successive cycles as indicated by the similar E_{trans} values for the two additional switching cycles (cycles 2 and 3). An estimate of the fraction of ROX$_a$ binding sites that remain active (r_{a}) for FRET switching is given by:

$$r_{\text{a}} = 1 - \frac{\mathcal{F}_{\text{ADoff}}}{\mathcal{F}_{\text{ADon}}}, \tag{5}$$

where $\mathcal{F}_{\text{ADon}}$ is f_{AD} evaluated for the system in the 'ON' state, and $\mathcal{F}_{\text{ADoff}}$ is f_{AD} evaluated for the system in the 'OFF' state. The averaged r_{a} value for successive 'OFF–ON' cycles is 0.45 ± 0.11. Hence, 45% of the ROX$_a$ binding sites remain active, which is one area that can be improved upon in future work.

4. Conclusion

We have demonstrated efficient and switchable DNA-mediated upconversion FRET by engineering an UCNP–ROX donor/acceptor excitonic system through implementing (1) a simple, one-step direct attachment of ssDNA to hydrophobic UCNPs, and (2) a ROX acceptor-DNA strand design that exploits the ability to both hybridize with the ssDNA biofunctionalized UCNPs and undergo toehold-mediated strand-displacement. Decreased donor–acceptor distance from the direct attachment resulted in a quantum efficiency indistinguishable from unity and superior FRET that produced energy conversion and energy transfer efficiencies of nearly 25%. Successive switching events were performed using toehold-mediated strand-displacement that, although only 45% of sites were actually switching, allowed cycling of the excitonic FRET switch's state to be performed through three complete 'OFF–ON' cycles. The FRET produced a clear quenching of the donor emission with a significant simultaneous increase in acceptor emission that has yet to be fully demonstrated in other work. In principle, the upconversion FRET scheme reported here can lead to more efficient artificial light harvesting systems and excitonic devices, be incorporated to enhance photovoltaic devices, and be utilized to produce novel nanomedical assays.

Acknowledgments

The authors thank the students, staff, and faculty within the Nanoscale Materials & Device group for valuable assistance with this work and Mr Lonnie Tustison of Custom Tooling Services (Boise, Idaho) for his aid in design and fabrication of laser filter mounts. The research was supported in part by: (1) NSF IDR No. 1014922, (2) a WM Keck Foundation Award, and (3) the Micron Technology MSE PhD Fellowship. The UCNPs were obtained from the Lawrence Berkeley National Laboratory's Molecular Foundry, which is supported by the Office of Science, Office of Basic Energy Sciences, of the US Department of Energy under Contract No. DE-AC02-05CH11231. We are appreciative of Dr Emory Chan of the Molecular Foundry for helpful discussions on UCNPs and IR lasers.

References

[1] Horton P, Ruban A V and Walters R G 1996 Regulation of light harvesting in green palnts *Annu. Rev. Plant Physiol. Plant Mol. Biol.* **47** 655–84
[2] Scholes G D, Fleming G R, Olaya-Castro A and van Grondelle R 2011 Lessons from nature about solar light harvesting *Nat. Chem.* **3** 763–74
[3] Yamazaki I, Mimuro M, Murao T, Yamazaki T, Yoshihara K and Fujita Y 1984 Excitation energy transfer in the light harvesting antenna system of the red alga porphyridium cruentum and the blue-green alga anacystis nidulans: analysis of time-resolved fluorescence spectra *Photochem. Photobiol.* **39** 233–40
[4] Schmidt am, Busch M, Müh F, El-Amine Madjet M and Renger T 2011 The eighth bacteriochlorophyll completes the excitation energy funnel in the fmo protein *J. Phys. Chem. Lett.* **2** 93–8
[5] Vyawahare S, Eyal S, Mathews K D and Quake S R 2004 Nanometer-scale fluorescence resonance optical waveguides *Nano Lett.* **4** 1035–9
[6] Dutta P K, Varghese R, Nangreave J, Lin S, Yan H and Liu Y 2011 DNA-directed artificial light-harvesting antenna *J. Am. Chem. Soc.* **133** 11985–93
[7] Spillmann C M and Medintz I L 2015 Use of biomolecular scaffolds for assembling multistep light harvesting and energy transfer devices *J. Photochem. Photobiol.* C **23** 1–24
[8] Graugnard E, Kellis D L, Bui H, Barnes S, Kuang W, Lee J, Hughes W L, Knowlton W B and Yurke B 2012 DNA-controlled excitonic switches *Nano Lett.* **12** 2117–22
[9] Cannon B L, Kellis D L, Davis P H, Lee J, Kuang W, Hughes W L, Graugnard E, Yurke B and Knowlton W B 2015 Excitonic and logic gates on DNA brick nanobreadboards *ACS Photonics* **2** 398–404
[10] Fenna R E and Matthews B W 1975 Chlorophyll arrangement in a bacteriochlorophyll protein from chlorobium limicola *Nature* **258** 573–7
[11] Tronrud D E, Schmid M F and Matthews B W 1986 Structure and x-ray amino acid sequence of a bacteriochlorophyll a protein from prosthecochloris aestuarii refined at 1.9 å resolution *J. Mol. Biol.* **188** 443–54
[12] Vulto S I E, Neerken S, Louwe R J W, de Baat M A, Amesz J and Aartsma T J 1998 Excited-state structure and dynamics in fmo antenna complexes from photosynthetic green sulfur bacteria *J. Phys. Chem.* B **102** 10630–5
[13] Ishizaki A and Fleming G R 2009 Theoretical examination of quantum coherence in a photosynthetic system at physiological temperature *Proc. Natl Acad. Sci. USA* **106** 17255–60
[14] Ishizaki A and Fleming G R 2012 Quantum coherence in photosynthetic light harvesting *Annu. Rev. Condens. Matter Phys.* **3** 333–61
[15] Page R H, Schaffers K I, Waide P A, Tassano J B, Payne S A, Krupke W F and Bischel W K 1998 Upconversion-pumped luminescence efficiency of rare-earth-doped hosts sensitized with trivalent ytterbium *J. Opt. Soc. Am.* B **15** 996–1008
[16] Haase M and Schäfer H 2011 Upconverting nanoparticles *Angew. Chem., Int. Ed. Engl.* **50** 5808–29
[17] Liu G 2015 Advances in the theoretical understanding of photon upconversion in rare-earth activated nanophosphors *Chem. Soc. Rev.* **44** 1635–52
[18] Chen G, Qiu H, Prasad P N and Chen X 2014 Upconversion nanoparticles: design, nanochemistry, and applications in theranostics *Chem. Rev.* **114** 5161–214
[19] Chen N-T, Cheng S-H, Liu C-P, Souris J, Chen C-T, Mou C-Y and Lo L-W 2012 Recent advances in nanoparticle-based förster resonance energy transfer for biosensing, molecular imaging and drug release profiling *Int. J. Mol. Sci.* **13** 16598–623
[20] DaCosta M V, Doughan S, Han Y and Krull U J 2014 Lanthanide upconversion nanoparticles and applications in bioassays and bioimaging: a review *Anal. Chim. Acta* **832** 1–33
[21] Zhang Y, Wei W, Das G K and Yang Tan T T 2014 Engineering lanthanide-based materials for nanomedicine *J. Photochem. Photobiol.* C **20** 71–96
[22] Gargas D J *et al* 2014 Engineering bright sub-10 nm upconverting nanocrystals for single-molecule imaging *Nat. Nanotechnology* **9** 300–5
[23] Zhou J, Liu Q, Feng W, Sun Y and Li F 2015 Upconversion luminescent materials: advances and applications *Chem. Rev.* **115** 395–465
[24] Bettinelli M, Carlos L and Liu X 2015 Lanthanide-doped upconversion nanoparticles *Phys. Today* **68** 38–44
[25] de Bettencourt-Dias A 2007 Lanthanide-based emitting materials in light-emitting diodes *Dalton Trans.* 2229–41
[26] Dong H, Sun L-D and Yan C-H 2015 Energy transfer in lanthanide upconversion studies for extended optical applications *Chem. Soc. Rev.* **44** 1608–34
[27] Eliseeva S V and Bunzli J-C G 2010 Lanthanide luminescence for functional materials and bio-sciences *Chem. Soc. Rev.* **39** 189–227
[28] van der Ende B M, Aarts L and Meijerink A 2009 Lanthanide ions as spectral converters for solar cells *Phys. Chem. Chem. Phys.* **11** 11081–95
[29] Zou W, Visser C, Maduro J A, Pshenichnikov M S and Hummelen J C 2012 Broadband dye-sensitized upconversion of near-infrared light *Nat. Photonics* **6** 560–4
[30] Vuojola J and Soukka T 2014 Luminescent lanthanide reporters: new concepts for use in bioanalytical applications *Methods. Appl. Fluoresc.* **2** 012001
[31] Xu H, Chen R, Sun Q, Lai W, Su Q, Huang W and Liu X 2014 Recent progress in metal–organic complexes for optoelectronic applications *Chem. Soc. Rev.* **43** 3259–302

[32] Carlos L D, Ferreira R A S, de Zea Bermudez V, Julian-Lopez B and Escribano P 2011 Progress on lanthanide-based organic–inorganic hybrid phosphors *Chem. Soc. Rev.* **40** 536–49
[33] Dong H, Sun L-D and Yan C-H 2015 Energy transfer in lanthanide upconversion studies for extended optical applications *Chem. Soc. Rev.* **44** 1608–34
[34] Liu G 2015 Advances in the theoretical understanding of photon upconversion in rare-earth activated nanophosphors *Chem. Soc. Rev.* **44** 1635–52
[35] Knox R S 2012 Förster's resonance excitation transfer theory: not just a formula *J. Biomed. Opt.* **17** 0110031–6
[36] Förster T 2012 Energy migration and fluorescence *J. Biomed. Opt.* **17** 0110021–210
[37] Peng X, Chen H, Draney D R, Volcheck W, Schutz-Geschwender A and Olive D M 2009 A nonfluorescent, broad-range quencher dye for förster resonance energy transfer assays *Anal. Biochem.* **388** 220–8
[38] Quach A D, Crivat G, Tarr M A and Rosenzweig Z 2011 Gold nanoparticle−quantum dot−polystyrene microspheres as fluorescence resonance energy transfer probes for bioassays *J. Am. Chem. Soc.* **133** 2028–30
[39] Ho D, Noor M O, Krull U J, Gulak G and Genov R 2013 Cmos spectrally-multiplexed fret-on-a-chip for DNA analysis *Biomedical Circuits and Systems, IEEE Transactions on* **7** 643–54
[40] Didenko V V 2001 DNA probes using fluorescence resonance energy transfer (FRET): designs and applications *Biotechniques* **31** 1106–21
[41] Heer S, Kömpe K, Güdel H U and Haase M 2004 Highly efficient multicolour upconversion emission in transparent colloids of lanthanide-doped nayf4 nanocrystals *Adv. Mater.* **16** 2102–5
[42] Yurke B, Turberfield A J, Mills A P, Simmel F C and Neumann J L 2000 A DNA-fuelled molecular machine made of DNA *Nature* **406** 605–8
[43] Berney C and Danuser G 2003 Fret or no fret: a quantitative comparison *Biophys. J.* **84** 3992–4010
[44] Cen Y, Wu Y-M, Kong X-J, Wu S, Yu R-Q and Chu X 2014 Phospholipid-modified upconversion nanoprobe for ratiometric fluorescence detection and imaging of phospholipase d in cell lysate and in living cells *Anal. Chem.* **86** 7119–27
[45] Jiang S and Zhang Y 2010 Upconversion nanoparticle-based fret system for study of sirna in live cells *Langmuir* **26** 6689–94
[46] Kuningas K, Ukonaho T, Päkkilä H, Rantanen T, Rosenberg J, Lövgren T and Soukka T 2006 Upconversion fluorescence resonance energy transfer in a homogeneous immunoassay for estradiol *Anal. Chem.* **78** 4690–6
[47] Liu Y, Tu D, Zhu H, Ma E and Chen X 2013 Lanthanide-doped luminescent nano-bioprobes: from fundamentals to biodetection *Nanoscale* **5** 1369–84
[48] Soukka T, Rantanen T and Kuningas K 2008 Photon upconversion in homogeneous fluorescence-based bioanalytical assays *Ann. N.Y. Acad. Sci.* **1130** 188–200
[49] Tu D, Liu L, Ju Q, Liu Y, Zhu H, Li R and Chen X 2011 Time-resolved fret biosensor based on amine-functionalized lanthanide-doped nayf4 nanocrystals *Angew. Chem., Int. Ed. Engl.* **50** 6306–10
[50] Chen Z, Chen H, Hu H, Yu M, Li F, Zhang Q, Zhou Z, Yi T and Huang C 2008 Versatile synthesis strategy for carboxylic acid −functionalized upconverting nanophosphors as biological labels *J. Am. Chem. Soc.* **130** 3023–9
[51] Ang L Y, Lim M E, Ong L C and Zhang Y 2011 Applications of upconversion nanoparticles in imaging, detection and therapy *Nanomedicine* (*London, England*) **6** 1273–88
[52] Kumar M and Zhang P 2009 Highly sensitive and selective label-free optical detection of DNA hybridization based on photon upconverting nanoparticles *Langmuir* **25** 6024–7
[53] Rantanen T, Järvenpää M-L, Vuojola J, Kuningas K and Soukka T 2008 Fluorescence-quenching-based enzyme-activity assay by using photon upconversion *Angew. Chem., Int. Ed. Engl.* **47** 3811–3
[54] Sun L, Gu J, Zhang S, Zhang Y and Yan C 2009 Luminescence resonance energy transfer based on β-$NaYF_4$:Yb,Er nanoparticles and tritc dye *Sci. China* B **52** 1590–5
[55] Vetrone F, Naccache R, Morgan C G and Capobianco J A 2010 Luminescence resonance energy transfer from an upconverting nanoparticle to a fluorescent phycobiliprotein *Nanoscale* **2** 1185–9
[56] Selvin P R, Rana T M and Hearst J E 1994 Luminescence resonance energy transfer *J. Am. Chem. Soc.* **116** 6029–30
[57] Bogdan N, Vetrone F, Roy R and Capobianco J A 2010 Carbohydrate-coated lanthanide-doped upconverting nanoparticles for lectin recognition *J. Mater. Chem.* **20** 7543–50
[58] Riuttamäki T, Hyppänen I, Kankare J and Soukka T 2011 Decrease in luminescence lifetime indicating nonradiative energy transfer from upconverting phosphors to fluorescent acceptors in aqueous suspensions *J. Phys. Chem.* C **115** 17736–42
[59] Yuan Y and Liu Z 2012 An effective approach to enhanced energy-transfer efficiency from up-converting phosphors and increased assay sensitivity *Chem. Commun.* **48** 7510–2
[60] Liu J, Cheng J and Zhang Y 2013 Upconversion nanoparticle based lret system for sensitive detection of mrsa DNA sequence *Biosens. Bioelectron.* **43** 252–6
[61] Cheng L, Yang K, Shao M, Lee S-T and Liu Z 2011 Multicolor *in vivo* imaging of upconversion nanoparticles with emissions tuned by luminescence resonance energy transfer *J. Phys. Chem.* C **115** 2686–92
[62] Hilderbrand S A, Shao F, Salthouse C, Mahmood U and Weissleder R 2009 Upconverting luminescent nanomaterials: application to *in vivo* bioimaging *Chem. Commun.* 4188–90
[63] Clegg R M, Murchie A I and Lilley D M 1994 The solution structure of the four-way DNA junction at low-salt conditions: a fluorescence resonance energy transfer analysis *Biophys. J.* **66** 99–109
[64] Rantanen T, Jarvenpaa M-L, Vuojola J, Arppe R, Kuningas K and Soukka T 2009 Upconverting phosphors in a dual-parameter lret-based hybridization assay *Analyst* **134** 1713–6
[65] Kumar M, Guo Y and Zhang P 2009 Highly sensitive and selective oligonucleotide sensor for sickle cell disease gene using photon upconverting nanoparticles *Biosens. Bioelectron.* **24** 1522–6
[66] Wang F and Liu X 2009 Recent advances in the chemistry of lanthanide-doped upconversion nanocrystals *Chem. Soc. Rev.* **38** 976–89
[67] Dewey T G and Hammes G G 1980 Calculation on fluorescence resonance energy transfer on surfaces *Biophys. J.* **32** 1023–35
[68] Wu T, Kaur S and Branda N R 2014 Energy transfer between amphiphilic porphyrin polymer shells and upconverting nanoparticle cores in water-dispersible nano-assemblies *Org. Biomol. Chem.* **13** 2317–22
[69] Wang Y, Wu Z and Liu Z 2012 Upconversion fluorescence resonance energy transfer biosensor with aromatic polymer nanospheres as the lable-free energy acceptor *Anal. Chem.* **85** 258–64
[70] Li L-L, Wu P, Hwang K and Lu Y 2013 An exceptionally simple strategy for DNA-functionalized up-conversion nanoparticles as biocompatible agents for nanoassembly, DNA delivery, and imaging *J. Am. Chem. Soc.* **135** 2411–4
[71] Watson J D and Crick F H C 1953 Molecular structure of nucleic acids: a structure for deoxyribose nucleic acid *Nature* **171** 737–8

[72] Wei B, Wang Z and Mi Y 2007 Uniquimer: software of *De Novo* DNA sequence generation for DNA self-assembly—an introduction and the related applications in DNA self-assembly *J. Comput. Theor. Nanosci.* **4** 133–49
[73] Zadeh J N, Steenberg C D, Bois J S, Wolfe B R, Pierce M B, Khan A R, Dirks R M and Pierce N A 2011 Nupack: analysis and design of nucleic acid systems *J. Comput. Chem.* **32** 170–3
[74] Lakowicz J R 1999 *Principles of Fluorescence Spectroscopy* 3rd edn (Berlin: Springer)
[75] Porrès L, Holland A, Pålsson L-O, Monkman A, Kemp C and Beeby A 2006 Absolute measurements of photoluminescence quantum yields of solutions using an integrating sphere *J Fluoresc.* **16** 267–73
[76] Karstens T K , K 1980 Rhodamine b as referrence substance for quantum yield *J. Phys. Chem.* **84** 1871–2
[77] Uddin M J and Marnett L J 2008 Synthesis of 5- and 6-carboxy-x-rhodamines *Org. Lett.* **10** 4799–801
[78] Eaton D F 1988 Reference materials for fluorescence measurement *Pure Appl. Chem.* **60** 1107